

# **Simplified indexes for the seismic assessment of masonry buildings: International database and validation**

P.B. Lourenço<sup>1,\*</sup>, D.V. Oliveira<sup>2</sup>, J.C. Leite<sup>3</sup>, J.M Ingham<sup>4</sup>, C. Modena<sup>5</sup>, F. da Porto<sup>6</sup>

1, \* Corresponding author. Professor, ISISE, Department of Civil Engineering, University of Minho, Azurém, P 4800-058 Guimarães, Portugal. Phone: +351 253 510 209, fax: +351 253 510 217, email: pbl@civil.uminho.pt

2 Associate Professor, ISISE, Department of Civil Engineering, University of Minho, Azurém, P 4800-058 Guimarães, Portugal. Email: danvco@civil.uminho.pt

3 PhD Student, ISISE, Department of Civil Engineering, University of Minho, Azurém, P 4800-058 Guimarães, Portugal. Email: joaoleite@civil.uminho.pt.

4 Professor, Department of Civil and Environmental Engineering, University of Auckland, Auckland, New Zealand. E-mail: j.ingham@auckland.ac.nz

5 Professor, Department of Structural and Transportation Engineering, University of Padova, via Marzolo 9, 35131 Padua, Italy. E-mail: modena@unipd.it

6 Assistant Professor, Department of Structural and Transportation Engineering, University of Padova, via Marzolo 9, 35131 Padua, Italy. E-mail: francesca.daporto@unipd.it

## **Abstract**

Heritage masonry buildings are particularly vulnerable to earthquakes because they are deteriorated and damaged, they were built with materials with low resistance, they are heavy and the connections between the various structural components are often insufficient. The present work details a simplified method of seismic assessment of large span masonry structures that was applied to a database of forty-four monuments in Italy, Portugal and Spain, providing lower bound formulas for different simplified geometrical indexes. Subsequently, the proposed thresholds are validated with data from the 2010-2011 Canterbury earthquakes, which includes forty-eight stone and clay brick masonry churches. Finally, fragility curves that can be used to estimate the damage as a function of the peak ground acceleration (PGA) are also provided.

## **Keywords**

Seismic assessment; earthquake damage; masonry churches; simplified indexes; fragility curves

## **1 Introduction**

A disaster is an event caused by nature or man that causes great physical damage, destruction or loss of life, or a drastic change in the natural environment. Danger is the level of threat to life, property or environment, but it is important to understand that danger is not correlated to damage, and that disasters are the result of poor risk management.

Risk management involves, first, the perception and communication of risk to society. It is then essential to have proper tools for assessment and diagnosis, but also to define a set of possible solutions, and their costs, to implement a risk mitigation strategy. Over the past 30 years, economic losses due to disasters have increased tenfold, while earthquakes caused 80,000 deaths / year in the last decade, see Figure 1. Studies indicate that investment in mitigation provides society an average of four times the amount invested [FEMA, 2011]. In addition to savings to society, the US Federal Treasury can redirect an average of 3.65 times the money spent on mitigation resulting from disaster relief costs and tax losses avoided. This result was published in December 2005 in a report prepared by the Multi-hazard Mitigation Council of the National Institute of Building Sciences, called “Natural Hazard Mitigation Saves” [MMC, 2005]. The report was the culmination of a 3-year, Congressionally-mandated independent study. Another interesting example is given by the World Bank [2010] and United Nations where a study about retrofitting of buildings to increase earthquake resiliency provides a cost-benefit ratio of up to eight, for a discount rate of 5%. Sanghi [2010], on the presentation of the same study, provides a benefit-cost ratio of 4.6 for earthquakes, based in Istanbul, and stressed the obvious fact that the world population exposed to earthquakes will rise dramatically from 2000 to 2050. As mitigation of the seismic risk in the existing built heritage implies a large

investment, it is necessary to set priorities and consider an extended period of time to get communities physically, socially and economically resilient.

Recognizing that it is not possible to accept a full loss but it is also impossible to ensure the absence of any damage when an extreme event occurs, it is important to be prepared for disasters and for subsequent retrieval. Many existing buildings are highly vulnerable because they are deteriorated and damaged, they were built with materials with low resistance, they are heavy and the connections between the various structural components are often insufficient. The required approach is known, being necessary to: (i) characterize the existing built heritage; (ii) perform simplified analysis at the territorial level to estimate the vulnerability and risk of this heritage; (iii) in cases identified with higher risk in the previous step, perform detailed analyzes to confirm the vulnerability and risk, (iv) define a plan with long-term intervention measures and their costs, taking into account the observed risk, (v) implement the plan, with periodic reviews of time and costs, considering the economic constraints and the costs incurred in actual interventions. It is also true that a strategy like this requires political and societal commitment to become reality.

As masonry is one of the most used materials of the built heritage, this paper aims at providing a simple and fast screening tool at territorial level for a first safety assessment of masonry structures. In case of urban areas, and in spite of their diversity, a common matrix can usually be established for the seismic areas, more structural than technological. This built heritage consists typically of low height buildings (up to three stories), moderate spans (maximum of four or five meters) and large thickness of the walls (less than 1/7 of the height) [Giuffrè, 1995]. This paper is however focused in churches, given: (a) their intrinsic greater structural vulnerability due to open plan, greater height to width ratio and, often, the presence of thrusting horizontal structures from vaulted ceilings and timber roofs; (b) the ample geometry survey drawings and documentation available. Moreover, in earthquake prone countries, churches and monuments have already been subjected to earthquakes, and sometimes survived them, meaning that these structures are historical testimonies and they represent full-scale testing data. This fact permits to discuss and, generally, to accept that these ancient structures

have been adjusted to local seismicity. The simplified method of analysis for large span heritage buildings introduced in [Lourenco and Roque, 2006] is applied here to a database of forty-four monuments in Italy, Portugal and Spain, providing lower bound formulas for six different simplified geometrical indexes. The first three indices are associated with in-plane effects and they mainly refer to the ideal case of ordinary masonry structures, whose seismic response is related to the model of equivalent frame behavior. In particular, the accuracy of a given index depends on the conditions of structural regularity (typical approach for reinforced concrete structures and steel structures): regularity in plan and height, rigid decks, small number of floors, good quality of the links (connections, curbs or chains, lintels). The result of these indices, however, highly depends on the box-like behavior of the building and hence on the possibility to actually achieve a global response. This condition is very difficult to achieve in masonry structures such as monumental churches, for which the non-linearity and geometrical out-of-plane effects (local out-of-plane mechanisms) frequently prevail. These effects are partly addressed here through the out-of-plane indices.

In addition, the 2010-2011 Canterbury (New Zealand) earthquakes allow validation of the proposed formulations with a real seismic input and observed damage, and also to define fragility curves that can be used to estimate the damage as a function of the peak ground acceleration (PGA).

## **2 Database of results for masonry large span structures**

Structural analysis of masonry structures encompasses several different approaches and a comprehensive review is given in [Lourenço, 2002], with a recent update for seismic analysis in [Marques and Lourenço, 2011] for masonry with box behavior and in [Lourenço et al., 2011] for masonry without box behavior. Depending on the level of accuracy and the simplicity desired, usually the following representations are possible: (a) micro-modeling, where the geometry of units and joints is directly considered and the constitutive laws are obtained experimentally; (b) macro-modeling, where units and joints are smeared out in the continuum

and the constitutive laws are obtained experimentally; (c) homogenization, where the micro-structure is handled mathematically in terms of geometry and material data to obtain a smeared continuum model; (d) structural component models, where constitutive laws of structural elements are directly provided in terms of internal forces such as shear force or bending moment (and related generalized displacements), instead of stresses and strains, see Figure 2.

The approach proposed in [Lourenco and Roque, 2006] aims at a much simpler, faster and lower cost procedure, being based on a simplified geometric approach for immediate screening of the large number of buildings at risk. The objectives are to compare simple geometrical data taking into account local seismic hazard (PGA), and to evaluate the possibility to adopt simple indexes (a numerical indicator deduced from observations and used as an indicator of a process or condition) related to geometrical data as a first (very fast) screening technique to define priority for further studies with respect to seismic vulnerability. These fast techniques are to be used without actually visiting the buildings, encompassing therefore a low accuracy. It is expected that the geometrical indexes could detect cases of serious risk and can define priority of studies in countries/locations without recent earthquakes.

The usage of simplified methods of analysis usually requires that the structure is regular and symmetric, that floors act as rigid diaphragms and that the dominant collapse mode is in-plane shear failure of the walls [Meli, 1998], as also discussed above. In general, these last two conditions are not met by ancient masonry structures, meaning that simplified methods should not be understood as a quantitative safety assessment but merely as a simple indicator of possible seismic performance of a building. The following simplified methods of analysis and corresponding indexes are considered as in-plane indexes (Index 1, Plan area ratio; Index 2, Area to weight ratio, Index 3, Base shear ratio) and out-of-plane indexes (Index 4, Slenderness ratio of columns; Index 5, Thickness to height ratio of columns; Index 6: Thickness to height ratio of perimeter walls). All indexes refer only to geometrical parameters. Factors that are not taken into account (albeit qualitatively) are the type of construction, the quality of the walls and the connections, and the presence of pushing structures. To address these factors would require in situ investigations, which are needed for the study of an individual building but can hardly be

used for a first screening technique at territorial level, or for post-earthquake disasters, given the quantity of damage and the fact that access to the inside of many buildings is impossible due to safety reasons.

These methods can be considered as an operator that manipulates the geometric values of the structural walls and columns and produces a scalar value. As the methods measure different quantities, their application to a large sample of buildings contributes to further enlightenment of their application. As stated above, a more rigorous assessment of the actual safety conditions of a building is necessary to have quantitative values and to define remedial measures, if necessary.

## 2.1 In-plane indexes

The simplest index to assess the safety of ancient constructions is the ratio between the area of the earthquake resistant walls in each main direction (transversal x and longitudinal y, with respect to the church nave) and the total plan area of the buildings. According to Eurocode 8 [Eurocode 8, 2004], walls should only be considered as earthquake resistant if the thickness is larger than 0.35 m, and the ratio between height and thickness is smaller than nine. The first index  $\gamma_{1,i}$  reads:

$$\gamma_{1,i} = A_{wi}/S \quad [-] \quad \text{Equation 1}$$

where  $A_{wi}$  is the area of the earthquake resistant walls in direction “i” and  $S$  is the total area of the building.

The non-dimensional index  $\gamma_{1,i}$  is the simplest one, being associated with the base shear strength. Special attention is required when using this index as it ignores the slenderness ratio of the walls and the mass of the construction. Eurocode 8 [Eurocode 8, 2004] recommends values up to 5-6% for regular structures with rigid floor diaphragms. In cases of high seismicity, a minimum value of 10% seems to be recommended for historical masonry buildings [Meli,

1998]. For simplicity sake, high seismicity cases can be assumed as those where the design ground acceleration for rock-like soils is larger than 0.20g.

Index 2 provides the ratio between the area of the earthquake resistant walls in each main direction (again, transversal x and longitudinal y) and the total weight of the construction, reading:

$$\gamma_{2,i} = A_{wi}/G \quad [L^2F^{-1}] \quad \text{Equation 2}$$

where  $A_{wi}$  is the plan area of earthquake resistant walls in the direction “i” and  $G$  is the quasi-permanent vertical action. This index is associated with the horizontal cross-section of the building, per unit of weight. Therefore, the height (i.e. the mass) of the building is taken into account, but a major disadvantage is that the index is not non-dimensional, meaning that it must be analyzed for fixed units. In cases of high seismicity, a minimum value of 1.2 m<sup>2</sup>/MN seems to be recommended for historical masonry buildings [Meli, 1998], but on the basis of a more recent work [Lourenco and Roque, 2006], a minimum value of 2.5 m<sup>2</sup>/MN is adopted for high seismicity zones.

Finally, the base shear ratio provides a safety value with respect to the shear safety of the construction. The total base shear for seismic loading ( $V_{Sd,base} = F_E$ ) can be estimated from an analysis with horizontal static loading equivalent to the seismic action ( $F_E = \beta G$ ), where  $\beta$  is an equivalent seismic static coefficient related to the design ground acceleration. It is recommended to use the value of PGA for  $\beta$  in historical masonry structures. The true value of  $\beta$  in a finer analysis depends on the failure mechanism. For local mechanisms a correction that takes into account the participation mass and the height of the center of gravity of the macro-block, together with a behavior coefficient, should be applied. The shear strength of the structure ( $V_{Rd,base} = F_{Rd}$ ) can be estimated from the contribution of all earthquake resistant walls  $F_{Rd,i} = \sum A_{wi}f_{vk}$ , where, according to Eurocode 6 [Eurocode 6, 2006],  $f_{vk} = f_{vk0} + 0.4\sigma_d$ . Here,  $f_{vk0}$  is the cohesion, which can be assumed equal to a low value or zero in the

absence of more information,  $\sigma_d$  is the design value of the normal stress and 0.4 represents the tangent of a constant friction angle,  $\phi$ , equal to 22°. The new index  $\gamma_3$  reads:

$$\gamma_{3,i} = F_{Rd,i}/F_E \quad [-] \quad \text{Equation 3}$$

If zero cohesion is assumed ( $f_{vk0} = 0$ ),  $\gamma_{3,i}$  is independent from the building height, reading:

$$\gamma_{3,i} = V_{Rd,i}/V_{sd} = A_{wi}/A_w \times \tan \phi / \beta \quad \text{Equation 4}$$

But for a non-zero cohesion, which is most relevant for low height buildings,  $\gamma_{3,i}$  reads:

$$\gamma_{3,i} = V_{Rd,i}/V_{sd} = A_{wi}/A_w \times [\tan \phi + f_{vk0}/(\gamma \times h)]/\beta \quad \text{Equation 5}$$

where  $A_{wi}$  is the area of earthquake resistant walls in direction “i”,  $A_w$  is the total area of earthquake resistant walls,  $h$  is the (average) height of the building,  $\gamma$  is the volumetric masonry weight,  $\phi$  is the friction angle of masonry walls and  $\beta$  is an equivalent static seismic coefficient. Here, it is assumed that the normal stress in the walls is only due to their self-weight, i.e.  $\sigma_d = \gamma \times h$ , which is on the safe side and is a very reasonable approximation for historical masonry building, usually made of thick walls.

Equation 5 must be used rather carefully, since the contribution of the cohesion can be very large. Here, a cohesion value of 0.05 N/mm<sup>2</sup> will be assumed. This non-dimensional index considers the seismicity of the zone, which is taken into account in the factor  $\beta$ . The building will be safer with increasing ratio (earthquake resistant walls/weight), i.e. larger relation ( $A_w/A_{wi}$ ) and lower heights. For this type of buildings and action, a minimum value of  $\gamma_{3,i}$  equal to one seems acceptable.

The adopted indexes measure rather different quantities and cannot be directly compared. Index 2 is dimensional, which means that it should be used with particular care. Index 1 and index 2 are independent of the design ground acceleration. Therefore, assuming that the buildings must have identical safety, these indexes should be larger with increasing seismicity. For indexes 1 and 2, the seismicity is taken into account by considering that the threshold value given above is valid for a PGA/g value of 0.25 and a linear variation with PGA/g is assumed, as illustrated in Figure 3, see also Eurocode 8 [Eurocode 8, 2004]. In contrast, index 3 should be constant in different seismic zones, as it considers the effect of seismicity. This index format is close to the traditional safety approach adopted for structural design, being the threshold value equal to 1, see Figure 3.

## 2.2 Out-of-plane indexes

Besides the three indexes given above, other key indexes related with structural performance were computed for the database under analysis. It is well known that traditional masonry structures usually fail out-of-plane as observed in earthquakes, e.g. [Doglioni et al., 1994], and shaking table tests, e.g. [Mendes and Lourenço, 2010]. Limit analysis using macro-blocks can be carried out to assess the seismic performance of partial collapses that occur due to seismic action, generally, with the loss of equilibrium of rigid bodies., see e.g. [Lourenço et al., 2011], but this detailed analysis is outside the scope of the present article.

Instead, three simple geometric ratios concerning the structural out-of-plane behavior of columns and walls were adopted, when applicable. Slenderness ratio  $\gamma_4$ , and thickness to height ratio of the columns  $\gamma_5$ , as well as thickness to height ratio of the perimeter walls  $\gamma_6$ , were analyzed, reading:

$$\gamma_4 = h_{col} / (I/A) \quad \text{Equation 6}$$

$$\gamma_5 = d_{col} / h_{col} \quad \text{Equation 7}$$

$$\gamma_6 = t_{wall}/h_{wall}$$

Equation 8

where  $h_{col}$  is the free height of the columns,  $I$  and  $A$  are the inertia and the cross section area of the columns, respectively,  $d_{col}$  is the (equivalent) diameter of the columns and  $t_{wall}$  and  $h_{wall}$  are the thickness and the (average) height of the perimeter walls, respectively. All of the out-of-plane indexes are dimensionless and do not consider the local seismicity. If identical safety factors for the monuments are assumed, these indexes should vary with increasing seismicity, namely index 4 should decrease and index 5 and index 6 should increase.

### 2.3 Investigation for European churches (in-plane indexes)

The above mentioned simplified methods were applied to a sample of forty-four Portuguese, Spanish and Italian monuments, selected according to the seismic zonation and to the availability of information, with the following objectives: (a) Validate the hypothesis of an empirical relation of the ancient builders, able to define an expeditious preliminary assessment of the seismic vulnerability of historical masonry buildings; (b) Validate the hypothesis of an empirical relation between architectural-structural characteristics of historical masonry buildings and seismicity; (c) Prioritize further investigations and possible remedial measures for the selected sample; (d) Extrapolate, from the results of the sample, the seismic vulnerability of ancient masonry buildings in those countries.

For application of the simplified analysis methods, it was assumed that all the masonry materials were similar, the volumetric weight of masonry was  $20 \text{ KN/m}^3$  and the weight of the roofs was equal to  $2.0 \text{ KN/m}^3$ . The results are graphically represented as a function of the local parameter  $\text{PGA/g}$  in Figure 4, along with the threshold above mentioned for each of the indexes, namely  $\gamma_{1,i} \leq 10\%$ ,  $\gamma_{2,i} \leq 2.5 \text{ m}^2/\text{MN}$  and  $\gamma_{3,i} \leq 1.0$  for a  $\text{PGA/g}$  of 0.25.

In terms of average values, index 1 presents lower values in the transversal direction (x) of the church nave, which is expected due to churches' geometry, although Italian indexes are quite similar in both directions. Index 1 does not show a clear variation with seismicity, even if it tends to grow roughly with increasing seismicity. When a comparison is made using the

proposed threshold, 25% of the churches violate it in the x direction and 9% violate it in the y direction, as expected, since the same criterion is used in both directions. This outcome means that the cases that might require further investigation are due to a deficient earthquake resistance mainly along the transversal direction of the church nave.

Index 2, although being inversely proportional to the height of the buildings, presents a situation similar to index 1. Again, the calculated values do not show a visible trend with respect to seismicity, however a slightly tendency associates the increase of index 2 with PGA increase. On average, index 2 also presents lower values in the x direction, justified again by churches' geometry. As a result, this index is violated by 39% and 30% of the monuments in x and y directions, respectively. This index is mainly violated by Spanish churches.

Index 3 shows an alarming decreasing variation with the PGA parameter. For moderate and high seismicity areas (PGA greater than 0.15g), index 3 is violated by all churches, in both directions. In spite of that, also for low seismicity areas, index 3 is not entirely fulfilled. As happened with both previous indexes, index 3 presents lower values in the x direction. Individually, 41% and 32% of the churches in the x and y directions violate index 3, respectively, which denotes a deficient earthquake resistance along both the transversal and longitudinal directions. Unexpectedly, this index assumes minimum values slightly lower than 0.15, in both directions, which is most likely associated with high vulnerable structures, probably unable to properly face an earthquake. This index is mainly violated by Italian churches.

In order to perform a preliminary screening and to prioritize deeper studies in historical masonry structures in earthquake prone countries, a possible approach is to identify the monuments for which all in-plane indexes are violated, at least in one direction. An alternative approach would be to consider the simultaneous violation of index 3 and another one of the two remaining indexes (1 or 2). Both criteria show that deficient resistance to earthquake loading is not only associated with high seismicity, as for most of the Italian churches identified above, but it can also happen in moderate seismicity areas, e.g. two Portuguese churches, or even in low seismicity areas, such as for the majority of the Spanish churches. Considering the first

criterion, 18% of the sample requires remedial measures or, at least, deeper investigations. However, if the second criterion is used, almost half of the sample (43%) exhibits deficient earthquake resistance.

#### **2.4 Investigation for European monuments (out-of-plane indexes)**

The values obtained for the three out-of-plane indexes, are graphically represented in Figure 5, for the entire sample, as a function of the local seismicity. Similarly to the in-plane indexes, the out-of-plane indexes do not show any clear relationship with seismicity. However, for a PGA greater than 0.15g, a possible trend may be established. It can be observed that index 4 (column's slenderness) tends to decrease with increasing seismicity and that both index 5 and index 6 seem to increase continuously with seismicity. These trends are depicted in Figure 5 by dashed lines and can be seen as possible first threshold proposals.

### **3 The Christchurch (New Zealand) earthquake and the performance of local churches**

The recent Christchurch earthquake (CHC) in New Zealand (NZ) has provided valuable data to evaluate the proposed empirical thresholds just presented. In order to study the behavior of the masonry and heritage buildings in the region affected by the Canterbury sequence of earthquakes, an international team of post-graduate students was deployed in CHC soon after the 22 February 2011 earthquake with coordination provided by the NZ Natural Hazards Research platform. Statistical analysis of the damage data gathered for 48 churches in the region is presented here, followed by safety evaluation data on the damage classification registered for each church by the NZ authorities. Only the in-plane indexes can be validated as the available information is insufficient to validate the out-of-plane indexes.

### 3.1 A brief description of the earthquake

The Canterbury region of New Zealand has been subjected to an intense seismic activity that started on 4 September 2010 at 4:35 pm, when a magnitude  $M_w$  7.1 earthquake struck the region. The epicenter was located near Greendale, 40 km west of CHC (see Figure 6), at a depth of about 10 km. The earthquake produced a ground-surface fault rupture with a length of nearly 30 km and during the ground motion the measured Peak Ground Acceleration (PGA) reached 0.82g for the horizontal component and 1.26g for the vertical component [Allen et al., 2010].

Almost 1500 aftershocks, with a magnitude of  $M_w$  5.0 or higher, were recorded [GeoNet, 2011a] from that day until 22 February 2011, when another major seismic event struck the region. At 12:51 pm an aftershock with a magnitude  $M_w$  6.3 and an epicenter located only 10 km south-east of the CHC and at a depth of 5 km, was felt throughout the entire Canterbury region (see Figure 7). More than 180 people lost their lives and a similar number were severely injured, and the PGA reached 1.7g for the horizontal component and 2.2g for the vertical component. High magnitude aftershocks did not stop in the February event and on 13 June 2011 another two large events occurred with magnitudes  $M_w$  of 5.7 and 6.3.

After the February event, the Central Business District (CBD) of CHC was partially destroyed and considered unsafe by the Ministry of Civil Defense and Emergency Management, which had it cordoned. A large number of heritage buildings, mostly constructed using unreinforced clay brick masonry, partially collapsed or were damaged beyond repair [Dizhur et al., 2011]. A building safety evaluation process was activated hours after each of the major events, as required by NZ legislation when a state of emergency is declared [New Zealand Legislation, 2002]. The process overview and guidelines are reported in [New Zealand Society for Earthquake Engineering, 2009] and were based on North American procedures developed by the Applied Technology Council [Applied Technology Council (ATC), 1989; Applied Technology Council (ATC), 1995]. The outcome of the process is the classification, followed by the fixing of a placard at the main entrance, of all the buildings into three color tags; with the following meaning: *green* if there were no restrictions to use of the building; *yellow* if there were safety concerns, restricting use of the building to short periods of time for essential

business; *red* if the building was clearly unsafe and therefore re-entry of the building was prohibited. Heritage buildings were also assessed following the process.

### **3.2 Church typologies and earthquake performance**

After becoming a colony of the British Empire in 1840, the demand for residential and community buildings increased due to the larger number of immigrant population [Russell and Ingham, 2010]. The wide availability of wood, and faster construction times, made timber the main construction material during this period. The subsequent prosperity led to the use of stone and clay brick in the construction of important public buildings such as churches. Therefore, these are the three most common materials used for the construction of NZ churches from the first quarter of the 20<sup>th</sup> century (see Figure 8). Almost all churches of the Canterbury region built before 1938 were assessed [Hamilton and Hamilton, 2008], leading to a total number of 112 church buildings contained within the database (see Figure 9). The exceptions were churches that were already demolished and churches that were damaged to such an extent that it was unsafe to perform the assessment.

A comprehensive statistical analysis of the churches including the in situ damage observed, the structural assessment classification assigned by the local authorities and a comparison with the structural classification used in Italy, where a specific survey form for churches is used, is given in [Leite et al., 2013]. More than half of the churches (57%) received a green placard from the structural inspectors (see Figure 10 a), but given the different dynamic characteristics of the three principal church typologies found in the Canterbury region as referred to above, the obtained data had to be analyzed for each individual typology. For the stone churches, more than half of the churches (52%) were assigned a red placard and only 16% of the churches had a green placard assigned (see Figure 10 b). Identically, Figure 10 c) shows that a red placard was assigned to 38% of the clay brick churches, while a yellow placard was assigned to 42% of those churches. The percentage of red placards assigned for the typology was smaller than the percentage assigned for the stone churches, but the sum of the red and yellow placards was similar for both masonry typologies and exceeded 80%. Figure 10 d) shows

that 94% of the timber churches were assigned a green placard. The single red placard assigned to this typology was due to non-structural damage, being mainly cracking of plaster. Therefore, a general comment on the overall performance of the churches is misleading, as timber churches had an excellent seismic performance, while the stone and clay brick churches clearly performed unsatisfactorily.

The masonry used to build the brick churches is of low quality, given the poor quality of the mortar used [Dizhur et al., 2011]. Still, there is a three dimensional bond of the wall leaves that provides a reasonable interlocking and partly prevents material disintegration, see Figure 11. Contrarily to the clay brick churches, which were all built with the same technique and similar materials, the stone churches vary considerably in composition. There are stone churches built with a stone leaf on the outside, a brick leaf inside and poor quality concrete between the leafs, see Figure 12, and there are stone churches built entirely with rubble masonry, see Figure 13, that are rather prone to material disintegration and out-of-plane expulsion . Now it remains to be discussed how the observed damage compares with the proposed in-plane thresholds.

#### **4 Validation thresholds with NZ data and fragility curves**

The assessment carried out after the CHC earthquake included the recording of the placard assigned to each church by the NZ National Authorities, a visual inspection (exterior and interior when possible and safe) with photographic documentation of the damage, see Figure 14, completion of the Italian survey form for damage in cultural heritage – churches [Civil Protection Department, 2006] and the geometrical measurement, in plan and height, using a distance meter laser. The thickness of the walls was obtained rather easily in the clay brick churches because the same type of brick and construction techniques were used. As for the stone churches, the heavily damaged churches with large cracks or local collapses allowed an easy measurement, while in the less damaged churches the measurement was done at the openings (windows and doors).

The weight, friction angle and cohesion of masonry are also needed in order to compute all three indexes. The same weight and friction angle values were considered for both typologies, 18 KN/m<sup>2</sup> and 22° respectively, while the cohesion value assumed for  $f_{vk0}$  was 0.05 N/mm<sup>2</sup>. Index 3 was also computed considering zero cohesion, recognizing the particularly high level of recorded vertical acceleration.

#### 4.1 Index computation and PGA for each church

The indexes related to the above mentioned simplified method of analysis were computed for all the stone and clay brick churches. The timber church typology was excluded since the performance was excellent and the proposed method is not applicable. The objective was to validate the proposed thresholds for each of the three in-plane indexes (in-plane area ratio, area to weight ratio, base shear ratio) by means of the PGA imposed to each church during the 22 February 2011 seismic event, acquired by the National Strong Ground Motion Network's equipment. Given the high number of instruments installed in structures and buildings [Canterbury Regional Strong-Motion Network, 2003], it was possible to associate the PGA recorded at a given location to a nearby church building. In most cases the distance between the church building and the accelerographs was less than 2 km, which ensures the quality of the produced data. Considering the latitude and longitude coordinates of each church and the horizontal PGA associated to it, it is possible to plot a contour map, see Figure 15, which shows that the measured PGAs almost reach 1.4 g for the churches located near the CBD of CHC, and then decrease non-uniformly as the churches are located further away.

Figure 16 presents the scatter plots of each index and the recorded horizontal PGA of the 22 February 2011 event for clay brick churches, as well as the proposed thresholds from Figure 3. Direction X and Y correspond, respectively, to the transversal and longitudinal directions regarding the main nave. The threshold for the first index is excellent, with all the *green* tagged churches above or near the line and only one yellow and one red church incorrectly identified. The *yellow* tagged church had only minor cracking with the exception of a large shear crack on one longitudinal wall of the main nave, see Figure 17. There were also

unstable non structural elements inside that could collapse during a stronger aftershock, which led the structural inspector to classify the church as *yellow*. The *red* tagged church was also a particular case, as it had pinnacles overhanging from the transversal walls, see Figure 18 (a), and therefore was unstable even for a low PGA. These elements were severely damaged or partially collapsed, see Figure 18 (b), compromising the connection between the transversal and longitudinal walls. The thresholds for index 2 and 3 also have acceptable results. The X (or transverse) direction provides better results in all three indexes, and this is the critical direction. The indexes are consistent even if they are not directly correlated. Index 3 exhibits the worse performance if cohesion is taken into consideration, with better results obtained for a zero cohesion, see Figure 16 (e) (f) (g) (h).

The thresholds for the stone churches are not as good as those for the clay brick churches, see Figure 19. For all indexes, and in both directions, there are *green* tagged churches subjected to a PGA equal or higher to 1g under the threshold, and *red* tagged churches subjected to a PGA lower than 0.125g above the threshold. The lack of homogeneity of the stone churches justifies the lack of agreement with the thresholds, as the seismic behavior of these churches is rather different. Monumental good quality stone churches can present a seismic behavior similar to clay brick churches, while rubble weak stone masonry lacks interlocking and disaggregates, even for low PGA values. Redefining the thresholds is not a solution and the stone church typology would possibly have to be divided in sub-categories, according to more specific construction details. As it will be shown next with the fragility curves, the response of the stone churches is rather peculiar. As for the clay brick churches, there is a better agreement with the threshold of index 3 if cohesion is not taken into consideration.

Finally, it is noted that indexes 4 and 5 are related to the columns and these structural components rarely exist in the church typologies in New Zealand. These indexes are therefore non-applicable. Index 6 is also hardly applicable for these churches as they have rather small spans and many buttresses.

## 4.2 Fragility curves

After the above computations, the assessed buildings were sorted following the damage index  $i_d$  assigned to each one [Leite et al., 2013] and the PGA that the buildings were subjected to on the 22 February event, Figure 20. The damage Index  $i_d$ , is based on the concept of *macroelements* [Doglioni et al., 1994]. These *macroelements* are subdivisions of the church based on architectural elements (such as facade, lateral walls, chapel, bell tower) which have an almost independent seismic behaviour at collapse, therefore simplifying the complex structure of most churches into several smaller and simpler elements. The concept is based on experience acquired from past earthquakes, and was later revised and applied to the inspection forms [Angeletti et al., 1997; Lagomarsino and Podestà, 2004] used by the Italian Civil Protection [Civil Protection Department, 2006].

Each data plot of Figure 20 was divided into three shaded areas obtained using the average PGA of the group and one standard deviation, iteratively defined to include 70% of the data. This clustering provides two empirical fragility curves, being one referred to as *slight-moderate*, obtained considering the percentage of *green* tagged churches within the respective shaded areas, while the second one, referred to as *extensive-complete*, considered the percentage of *green* and *yellow* tagged churches in the same groups. Figure 21 shows the empirical fragility curves for stone and clay brick churches, individually and merged in a single group. The higher vulnerability of stone churches is clear, with almost 50% of the churches having important damage and over 75% of the churches having some damage for a PGA value of 0.25g. For brick similar values of damage occur for about 0.6g.

The fragility curves presented are inadequate to estimate the global losses in the case of important damage. For this purpose the lognormal distribution was fitted to the observed data [Singhal and Kiremidjian, 1996]. Several attempts were made but it was observed that the fit was far from perfect, providing unrealistic values for the extensive-complete damage, with low percentages of failure at higher PGAs. In addition, for slight-moderate damage, the curves are close to 100%, meaning that the use of the three data points can be unreliable. Finally, the following procedure was used, adopting the first two points in the fragility curves: (a) a

lognormal distribution was fitted to the data points; (b) the lognormal cumulative distribution function was set to pass in the average quantile; (c) the standard deviation (measured by  $\beta$ ) was obtained by the least square method for the slight-moderate sample, being the same  $\beta$  used for the extensive-complete damage. The fitted fragility curves are plotted in Figure 22, where a  $\beta$  equal to 1.3, 0.8 and 1.1, was found respectively for stone masonry, clay brick masonry and the entire sample. The higher vulnerability of stone churches is again demonstrated by the fitted fragility curves.

It is now assumed that the values of 5%, 50% and 95% quantiles are the lowest expected, the average, and the highest expected damage. For stone churches, it is expected that 50% receive a *yellow* tag for a PGA of 0.1g and a *red* tag for a PGA of 0.35g. For clay brick churches, it is expected that 50% receive a *yellow* tag for a PGA of 0.25g and a *red* tag for a PGA of 0.55g. For stone churches, it is expected that they all receive a *yellow* tag for a PGA of 0.65g and a *red* tag for a PGA of 3g. For clay brick churches, it is expected that they all receive a *yellow* tag for a PGA of 0.95g and a *red* tag for a PGA of 2.2g. Finally, for stone churches, it is expected that *yellow* tags appear for any seismic event and *red* tags appear for PGAs over 0.05g. For clay brick churches, it is expected that *yellow* tags appear for PGAs over 0.07g and *red* tags appear for PGAs over 0.15g.

In general for masonry churches, *yellow* tags are not expected for PGAs lower than 0.05g and *red* tags are not expected for PGAs lower than 0.1g. For PGAs of 0.15g and 0.5g, half of the churches are expected to be *yellow* and *red* tagged, respectively. For PGAs of 1g and 3g, all churches are expected to be *yellow* and *red* tagged, respectively.

## 5 Conclusions

The present work details the application of a simplified method for seismic assessment of large span masonry structures for a database of churches in Italy, Portugal and Spain, with further validation to a database gathered in Christchurch, New Zealand, after the 22 February 2011 earthquake. The first database includes forty-four churches, with in-plane and out-of-plane

simplified indexes. The second database includes forty-eight stone and clay brick masonry churches in New Zealand, to which only the in-plane indexes could be calculated.

The first index, being the plan area ratio, seems to provide very good results for clay brick churches, while the second index, being the area to weight ratio, and the third index, being the base shear ratio, also have acceptable results. The third index exhibits acceptable results only if the cohesion of masonry is not taken into consideration. The results for stone churches are inadequate, mainly due to their lack of homogeneity, since the database includes both monumental good quality masonry churches and rubble weak stone masonry with poor bond.

The present work also provides fragility curves for masonry churches based on the structural classification obtained during the safety evaluation process and the recorded PGA of each church. According to the results obtained, in general, *yellow* tags are not expected for PGAs lower than 0.05g and *red* tags are not expected for PGAs lower than 0.1g. For PGAs of 0.15g and 0.5g, half of the churches are expected to be *yellow* and *red* tagged, respectively. For PGAs of 1g and 3g, all churches are expected to be *yellow* and *red* tagged, respectively.

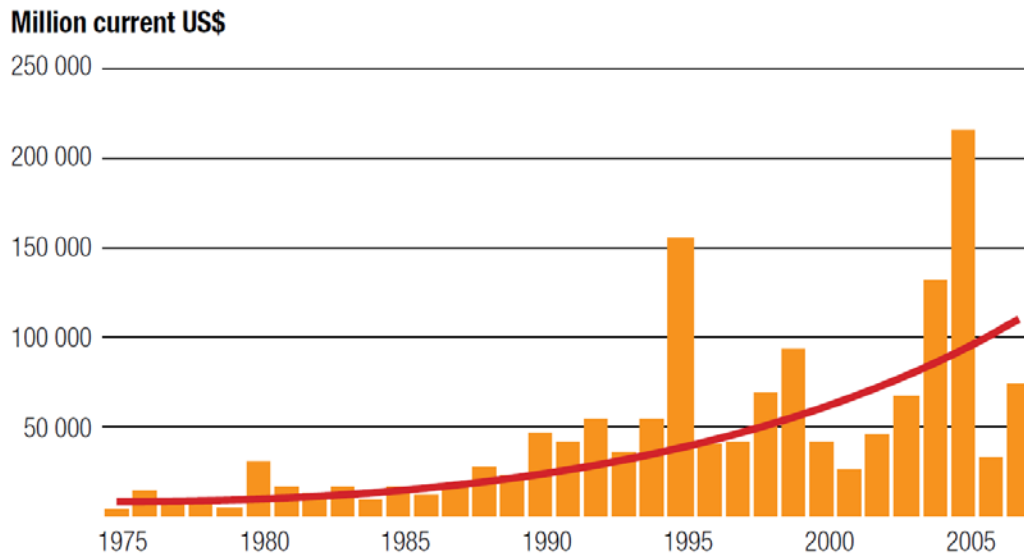
## 6 References

- Allen, J., Ashford, S., Bowman, E., Bradley, B., Cox, B., Cubrinovski, M., Green, R. A., Hutchinson, T., Kavazanjian, E., Orense, R., Pender, M., Quigley, M., and Wotherspoon, L. [2010] "Geotechnical Reconnaissance of the 2010 Darfield (Canterbury) Earthquake", *Bulletin of the New Zealand Society for Earthquake Engineering* 43 (4), 243-320.
- Angeletti, P., Ferrini, and Lagomarsino, S. [1997] "Survey and evaluation of the seismic vulnerability of the churches: and application in Lunigiana and Garfagnana (in Italian)", *Proc. of the 8th National Conference: Earthquake Engineering in Italy, Palermo*, 1077-1084.
- Applied Technology Council (ATC) [1989] "ATC-20: Procedures for Post-earthquake Safety Evaluation of Buildings ATC-20" Redwood City, CA, pp. 152.
- Applied Technology Council (ATC) [1995] "ATC-20-2: Addendum to the ATC-20 Post-earthquake Building Safety Procedures" Redwood City, CA, pp. 95.
- Canterbury Regional Strong-Motion Network. "Canterbury Seismic Instruments" [2003] Available from <http://www.csi.net.nz/profile.html>
- Civil Protection Department [2006] "Scheda per il rilievo del danno ai beni culturali - Chiese."
- Dizhur, D., Ingham, J., Moon, L., Griffith, M., Schultz, A., Senaldi, I., Magenes, G., Dickie, J., Lissel, S., Centeno, J., Ventura, C., Leite, J., and Lourenco, P.B. [2011] "Performance of Masonry Buildings and Churches in the 22 February 2011 Christchurch Earthquake," *Bulletin of the New Zealand Society for Earthquake Engineering* 44 (4), 279-296.
- Doglioni, F., Moretti, A., Petrini, V., and Angeletti, P. [1994] *Le chiese e il terremoto: dalla vulnerabilità constatata nel terremoto del Friuli al miglioramento antisismico nel restauro, verso una politica di prevenzione*, Trieste, Italy: Edizioni Lint.
- Eurocode 6 [2006] "Eurocode 6 - Design of masonry structures - Part 1-1: General rules for reinforced and unreinforced masonry structures (EN 1996-1-1), European Committee of Standardization" Brussels, Belgium.
- Eurocode 8 [2004] "Design of structures for earthquake resistance - Part 1: General rules, seismic actions and rules for buildings (EN 1998-1), European Committee of Standardization " Brussels, Belgium.
- FEMA [2011] Fact sheet: Mitigation's value to society, Federal Emergency Management Agency.
- GeoNet. "Aftershocks" [2011a] accessed 27/01/2012 Available from <http://www.geonet.org.nz/canterbury-quakes/aftershocks/>
- GeoNet. "Historic Earthquakes" [2011b] accessed 27/01/2012 Available from <http://www.geonet.org.nz/earthquake/historic-earthquakes/index.html>

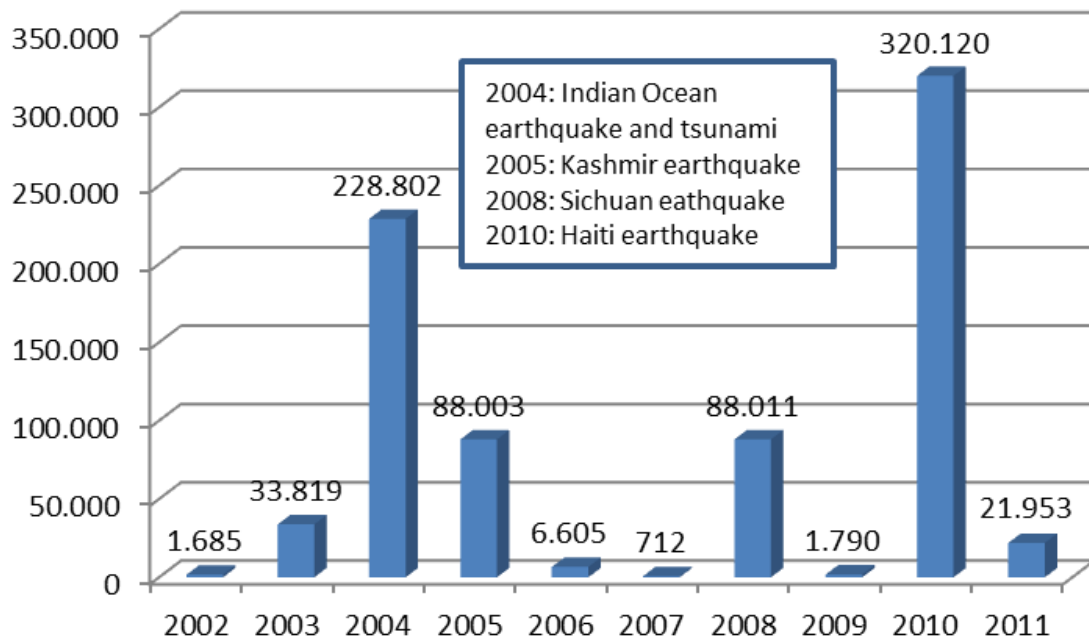
- Giuffrè, A. [1995] "Seismic damage in historic town centers and attenuation criteria", *Annali di Geofisica*, 38(5-6), 837-843.
- Hamilton, D., and Hamilton, J. (2008). *Early churches in and around Christchurch*, Christchurch: Judith and Derek Hamilton.
- Lagomarsino, S., and Podestà, S. [2004] "Seismic Vulnerability of Ancient Churches: I. Damage Assessment and Emergency Planning," *Earthquake Spectra* 20 (2), 377-394.
- Leite, J., Ingham, J. M., and Lourenço, P. B. [2013] "Statistical Assessment of Damage to Churches Affected by the 2010-2011 Canterbury (New Zealand) Earthquake Sequence," *Journal of Earthquake Engineering* 17 (1), 73-97.
- Lourenço, P. B., and Roque, J. A. [2006] "Simplified indexes for the seismic vulnerability of ancient masonry buildings", *Construction and Building Materials* 20 (2006), 200-208.
- Lourenço, P.B. [2002] "Computations of historical masonry constructions", *Progress in Structural Engineering and Materials*, 4(3): 301-319.
- Lourenço, P.B., Mendes, N., Ramos, L.F., Oliveira, D.V. [2011] "Analysis of masonry structures without box behavior", *International Journal of Architectural Heritage*, 5(4-5): 369-382.
- Marques, R., Lourenço, P.B. [2011] "Possibilities and comparison of structural component models for the seismic assessment of masonry buildings", *Computers and Structures*, 89 (21-22): 2079-2091.
- Mendes, N., Lourenço, P.B. [2010], Seismic assessment of masonry "Gaioleiros" buildings in Lisbon, Portugal, *Journal of Earthquake Engineering*, 14: 80-101.
- Meli, R. [1998] *Structural engineering of historical buildings (in Spanish)*, Mexico-City: Fundación ICA.
- MMC [2005] *Natural Hazard Mitigation Saves: An Independent Study to Assess the Future Savings from Mitigation Activities. Volume 1 – Findings, Conclusions and Recommendations. Volume 2 – Study Documentation*, Multihazard Mitigation Council of the National Institute of Building Sciences.
- New Zealand Legislation. "Civil Defence Emergency Management Act 2002" [2002] accessed 27/01/2012 Available from <http://www.legislation.govt.nz/act/public/2002/0033/latest/DLM149789.html>
- New Zealand Society for Earthquake Engineering [2009] "Building Safety Evaluation During a State of Emergency - Guidelines for Territorial Authorities."
- Russell, A., and Ingham, J. [2010] "Prevalence of New Zealand's Unreinforced Masonry Buildings." *Bulletin of the New Zealand Society for Earthquake Engineering* 43 (3, Sept.), 182-201.
- Sanghi, A. [2010] Presentation on "Natural hazards, unnatural disasters: The economics of effective prevention", The World Bank.

- Singhal, A., and Kiremidjian, A. S. [1996] "Method for probabilistic evaluation of seismic structural damage," *Journal of Structural Engineering* 122 (12), 1459-1467.
- U.S.G.S. [2012] U.S. Geological Survey, accessed 27/01/2012 Available from <http://www.usgs.gov/>.
- UNISDR [2009] Global assessment report on disaster risk reduction, United Nations International Strategy for Disaster Reduction Secretariat, ISBN 9789211320282, 207 pp.
- World Bank [2010] Natural hazards, unnatural disasters: The economics of effective prevention, The World Bank and The United Nations.

## Figures



(a)



(b)

Figure 1 - Effects of disasters: (a) Economic losses associated with natural disasters [UNISDR, 2009], (b) Number of deaths in the last ten years [U.S.G.S., 2012].

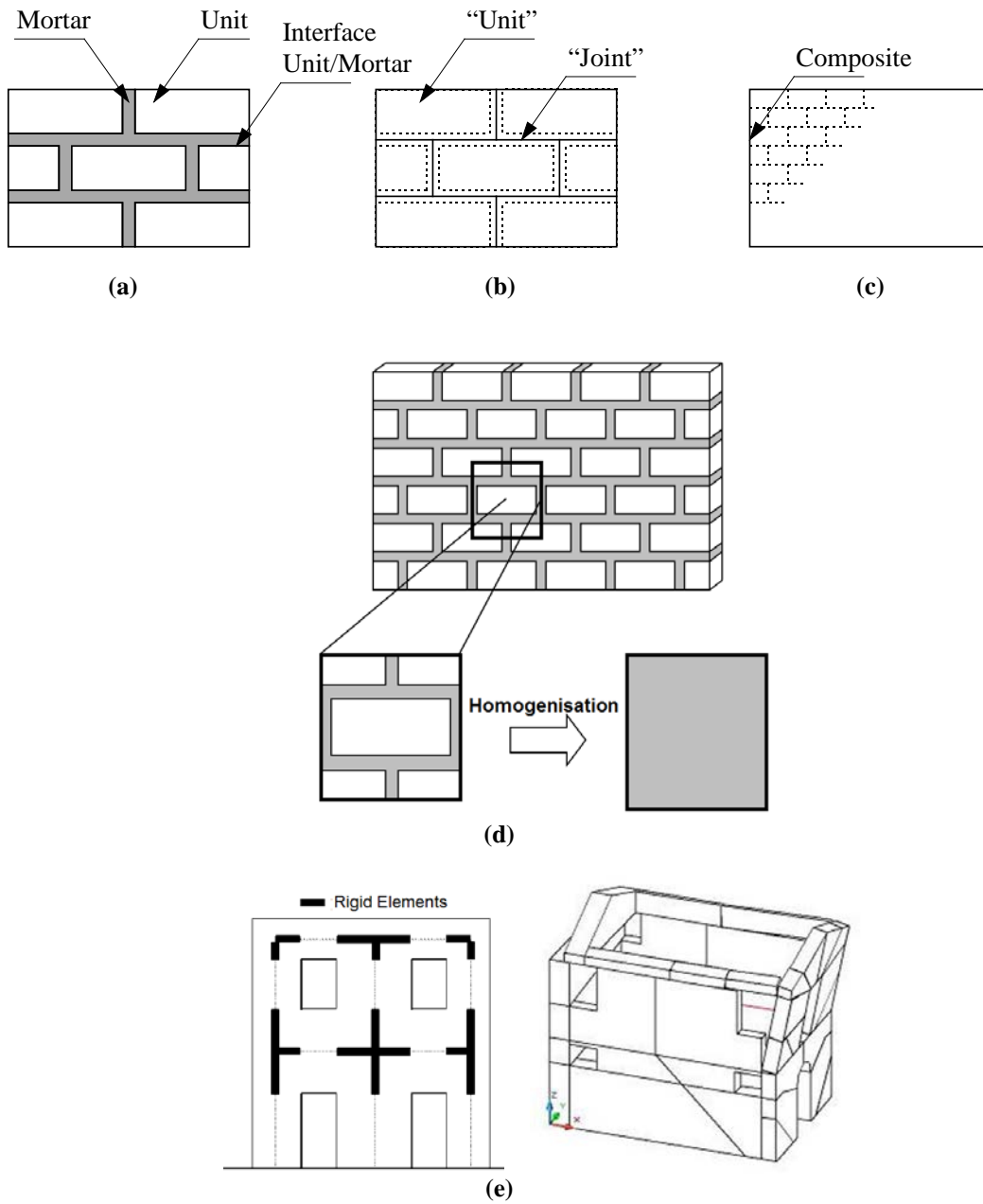


**Figure 2 - Modeling approaches for masonry: (a) representation of regular staggered or running bond masonry; (b) micro-modeling; (c) macro-modeling; (d) homogenization; (e) illustrative structural component models, with beam elements or macro-blocks.**

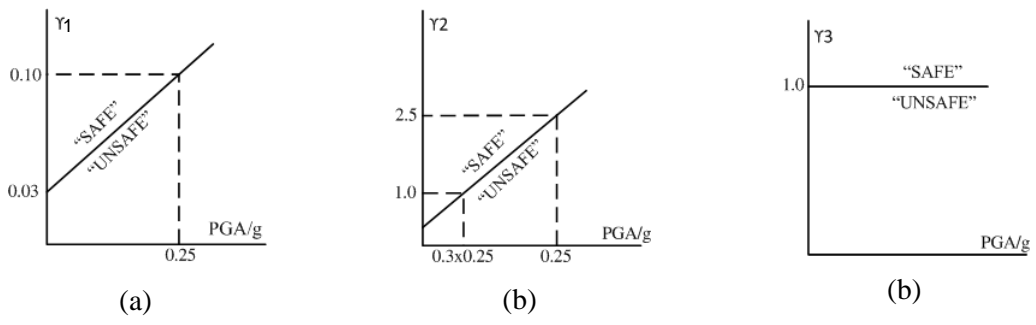
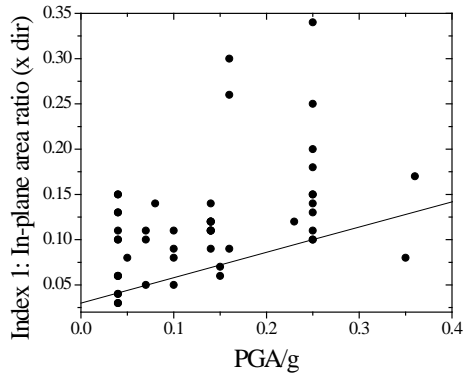
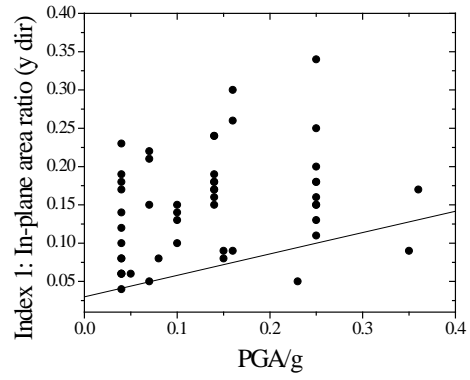


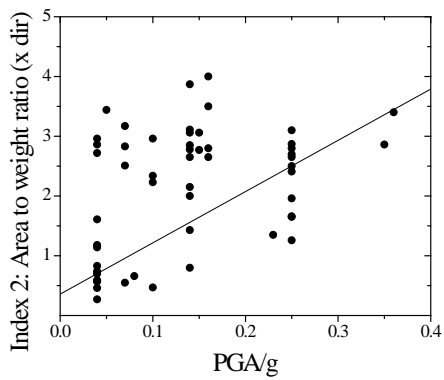
**Figure 3 – Assumed thresholds for indexes 1, 2 and 3 as a function of PGA/g, (a) index 1, (b) index 2, (c) index 3**



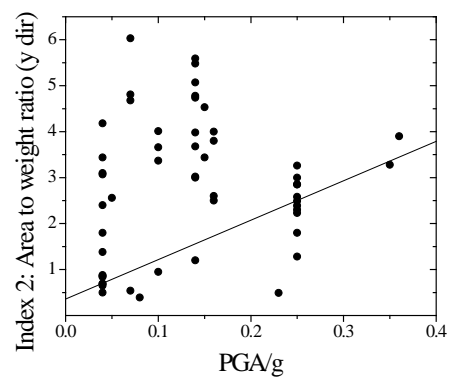
(a)



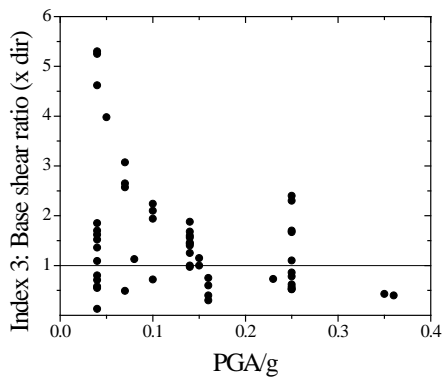
(b)



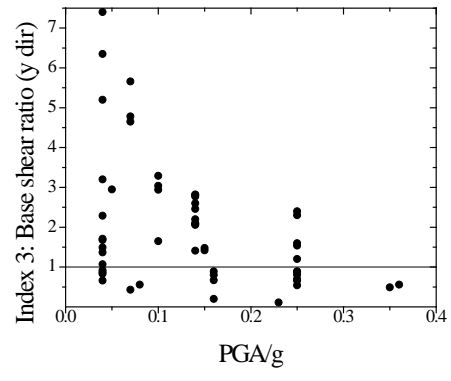
(b)



(c)

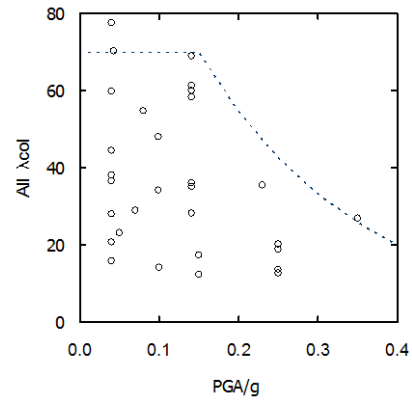


(d)

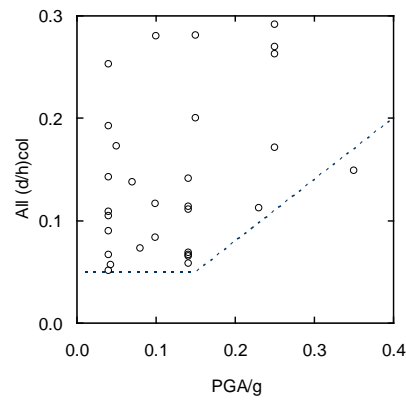


(e)

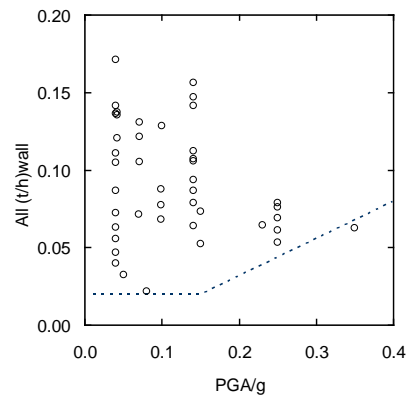
Figure 4 – Relationship between in-plane indexes and PGA/g, for the entire sample: direction x, (a) index 1, (b) index 2, (c) index 3; direction y, (c) index 1, (d) index 2, (e) index 3.



(a)



(b)

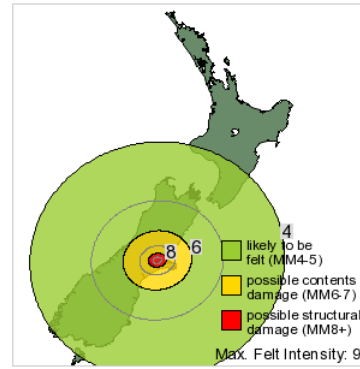


(c)

Figure 5 - Relationship between out-of-plane indexes and  $PGA/g$ , for the entire sample: (a) index 4; (b) index 5; (c) index 6.



(a)

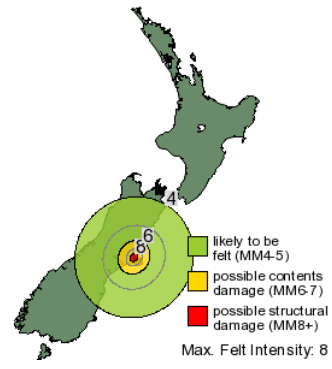


(b)

Figure 6 - Details of the 4 September 2010 earthquake [GeoNet, 2011b]: (a) earthquake location map; (b) isoseismal map.



(a)



(b)

Figure 7 - Details of the 22 February 2011 earthquake [GeoNet, 2011b]: (a) earthquake location map; (b) isoseismal map.



(a)

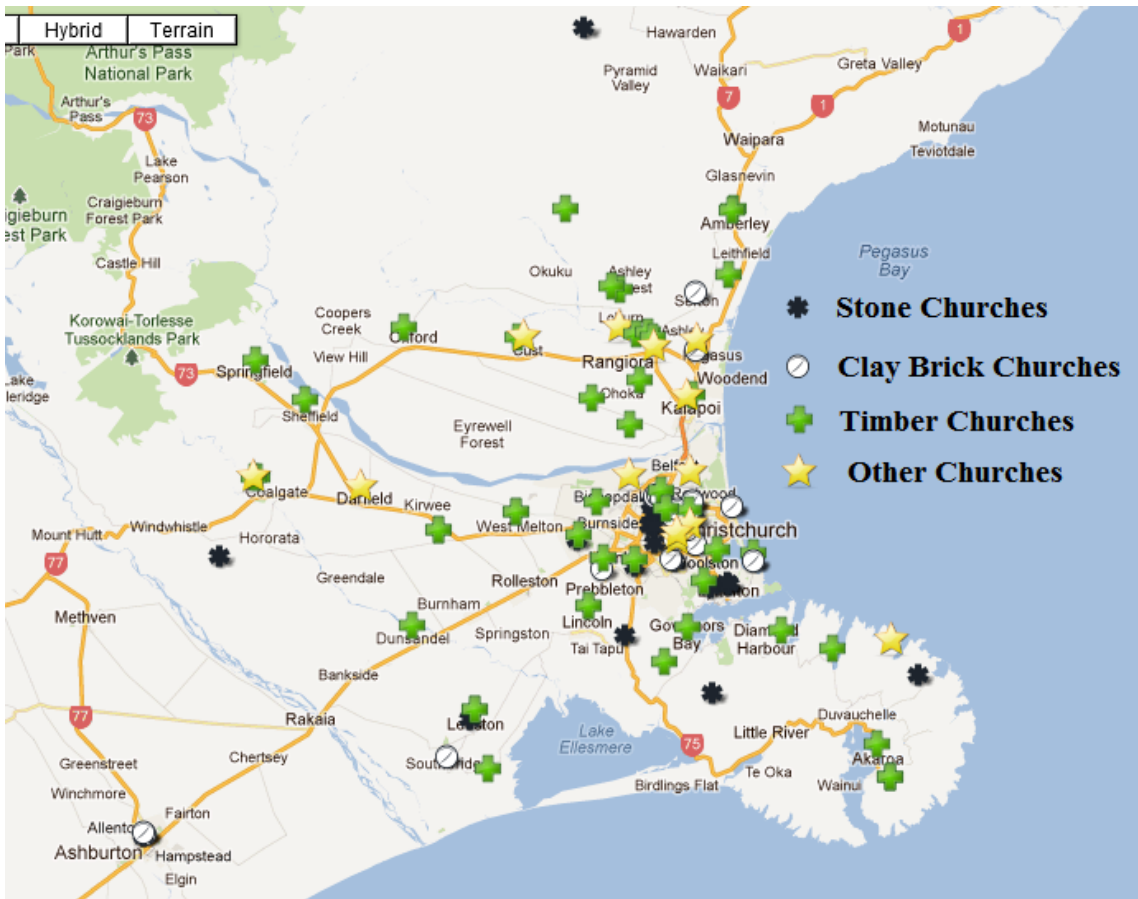


(b)

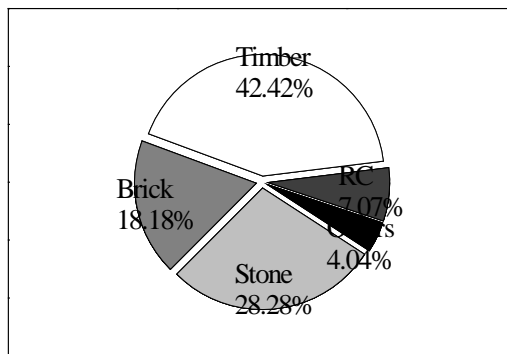


(c)

**Figure 8 - Church typologies found in the Canterbury region: (a) timber church of St Andrews, Merivale, 1857; (b) stone church of St Peters, Upper Riccarton, 1876; (c) clay brick church of Our Lady Star of the Sea, Sumner, 1912.**

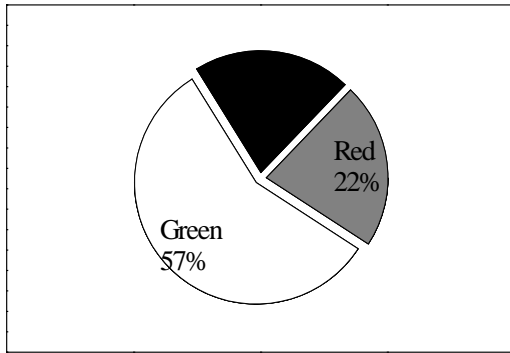


(a)

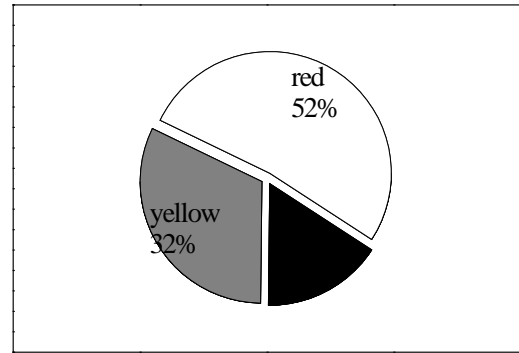


(b)

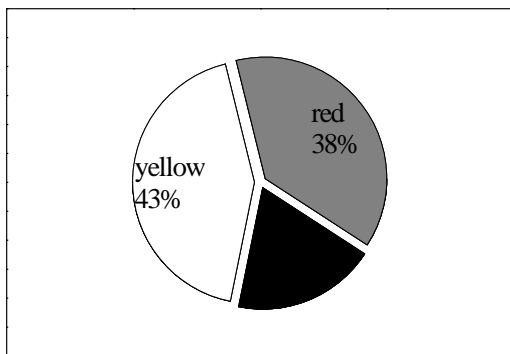
Figure 9 – Surveyed churches in the Canterbury District of New Zealand, (a) location; (b) typologies.



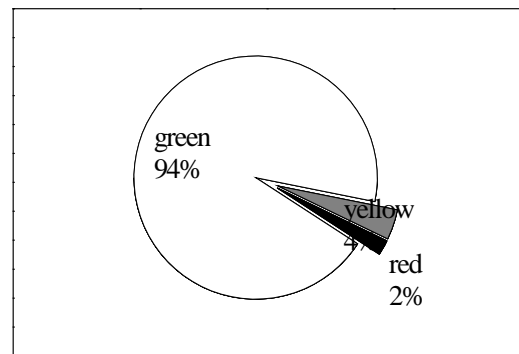
(a)



(b)



(c)



(d)

**Figure 10 – (a) placard classification for all the assessed churches; (b) placard classification for the stone churches; (c) placard classification for the clay brick churches; (d) placard classification for the timber churches.**



**Figure 11 - Detail of the three dimensional bond of the clay brick walls (Church of the Good Shepherd, Phillipstown).**



**Figure 12 – Different masonry leaves in stone churches (Rose Historic Chapel, Christchurch CBD), with stone outside and brick inside.**



(a)



(b)

**Figure 13 – Stone church with rubble masonry walls: (a) Holy Trinity, Lyttelton; (b) St. Cuthberts, Governors Bay.**



(a)



(b)

**Figure 14 – Visual inspections of churches: (a) interior inspection (St. James, stone, Riccarton); (b) exterior inspection only due to safety reasons (St. Josephs, stone, Lyttlelton).**

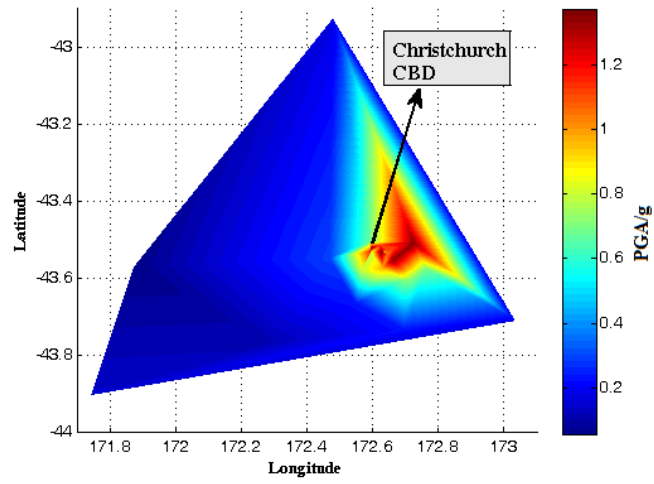
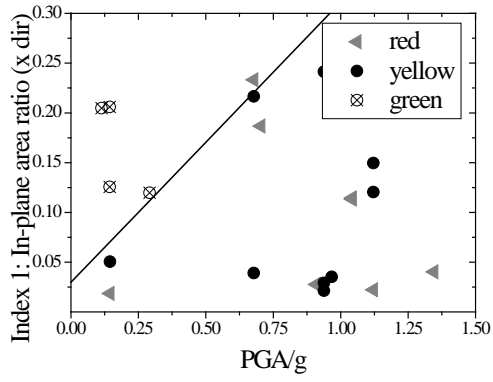
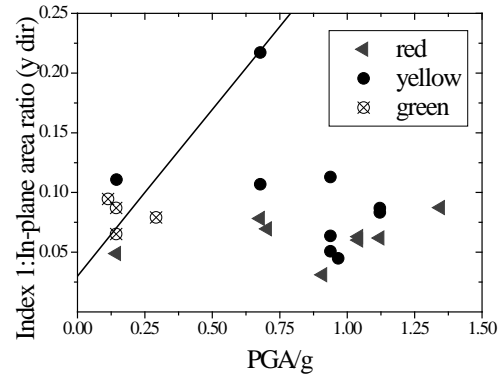


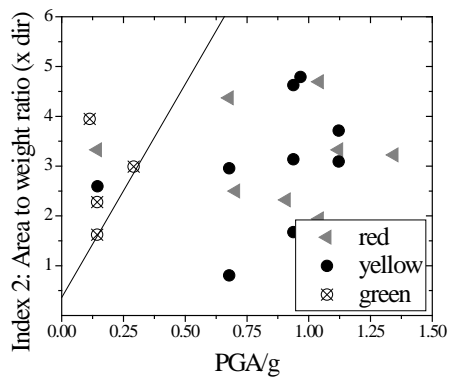
Figure 15 - PGA distribution of the assessed churches.



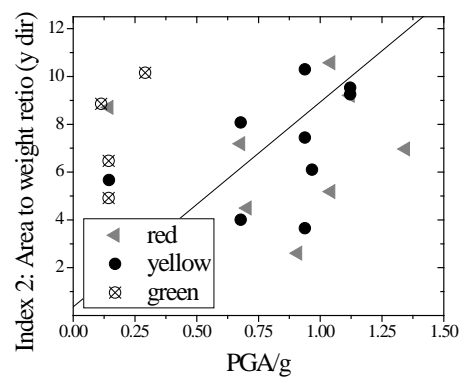
(a)



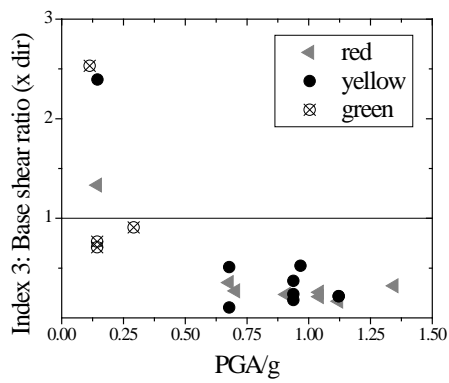
(b)



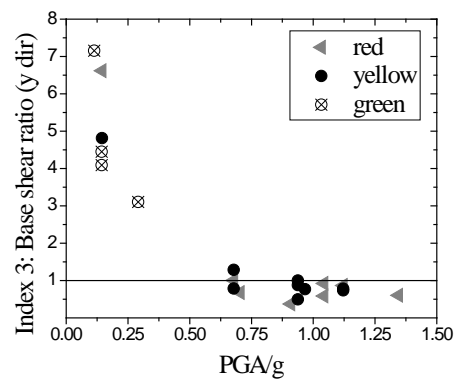
(c)



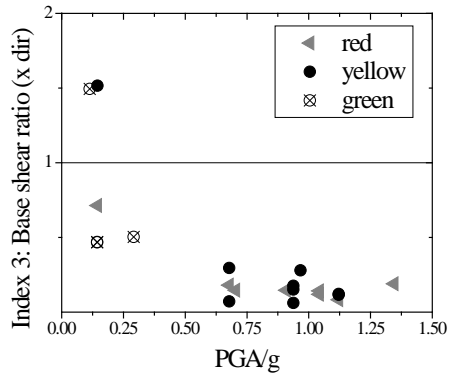
(d)



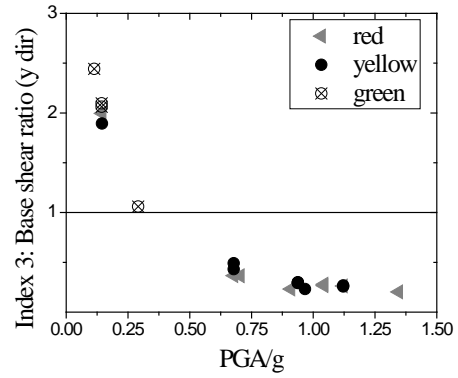
(e)



(f)



(g)



(h)

Figure 16 – Clay brick churches: (a) index 1: In-plane area ratio in the x (transversal) direction; (b) index 1: In-plane area ratio in the y (longitudinal) direction; (c) index 2: Area to weight ratio in the x (transversal) direction; (d) index 2: Area to weight ratio in the y (longitudinal) direction; (e) index 3: Base to shear ratio, taking cohesion into consideration, in the x (transversal) direction; (f) index 3: Base to shear ratio, taking cohesion into consideration, in the y (longitudinal) direction; (g) index 3: Base to shear ratio, considering zero cohesion, in the x (transversal) direction; (h) index 3: Base to shear ratio, considering zero cohesion, in the y (longitudinal) direction.



**Figure 17 – Large shear crack in the lateral wall of St. Luke’s Presbyterian church (clay brick, Sefton).**

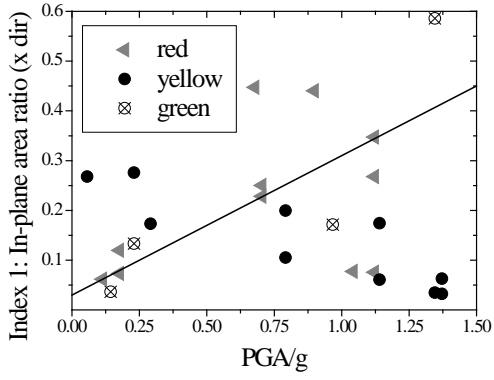


(a)

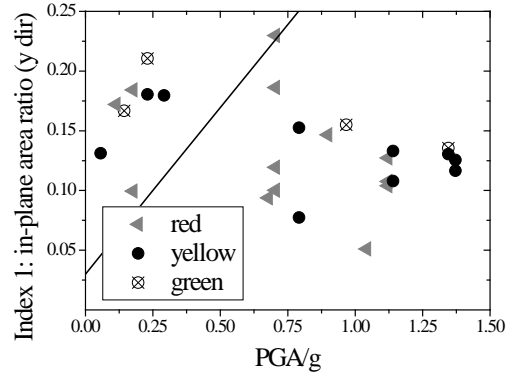


(b)

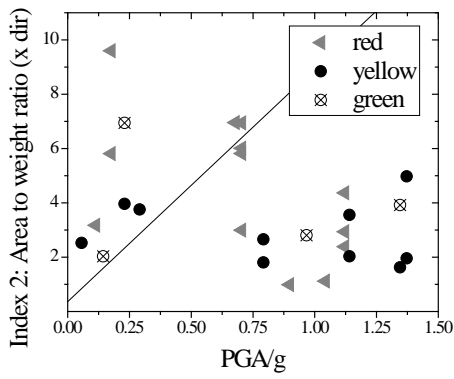
**Figure 18 – Damage in Woodend Methodist church (clay brick, Woodend): (a) pinnacles in each edge of the transversal walls of the main nave; (b) detail of a partially collapsed pinnacle with provisional reinforcement.**



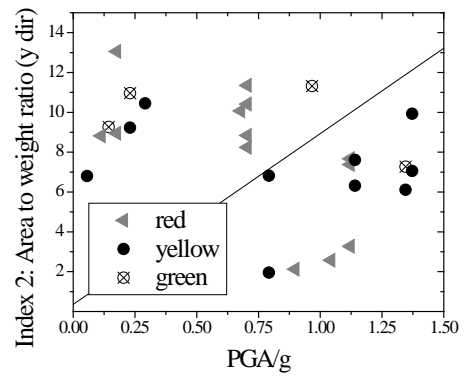
(a)



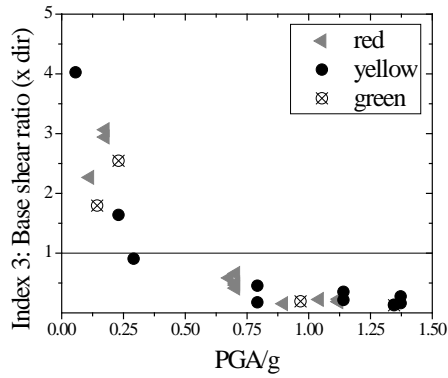
(b)



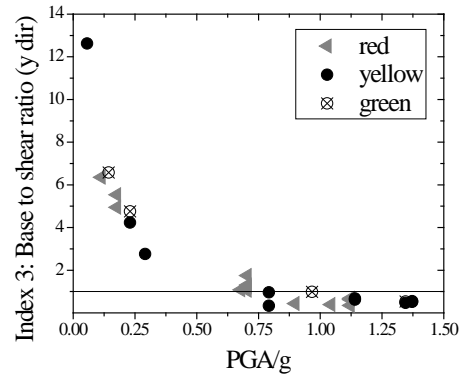
(c)



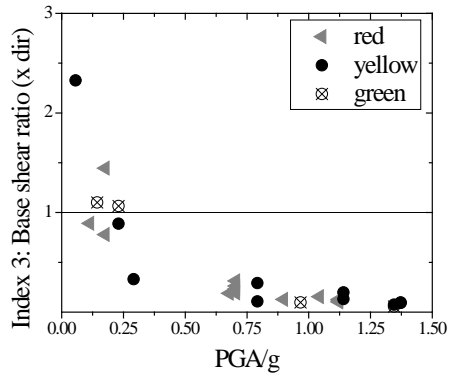
(d)



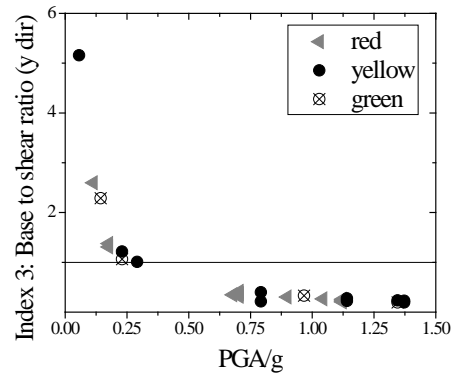
(e)



(f)

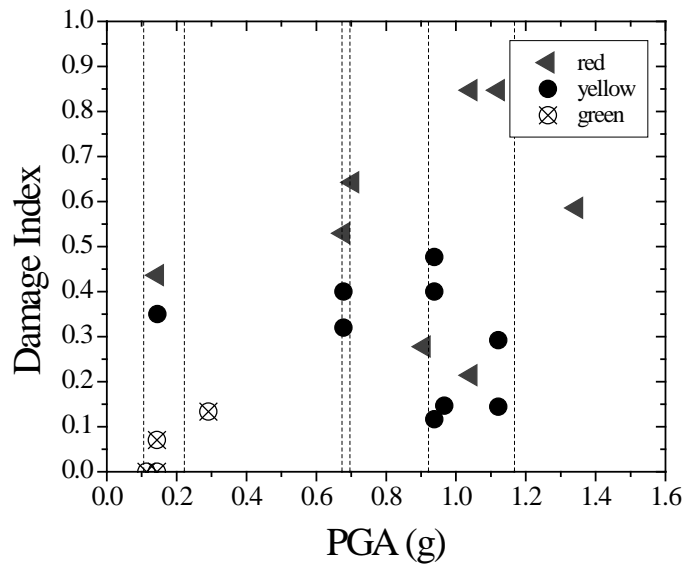


(g)

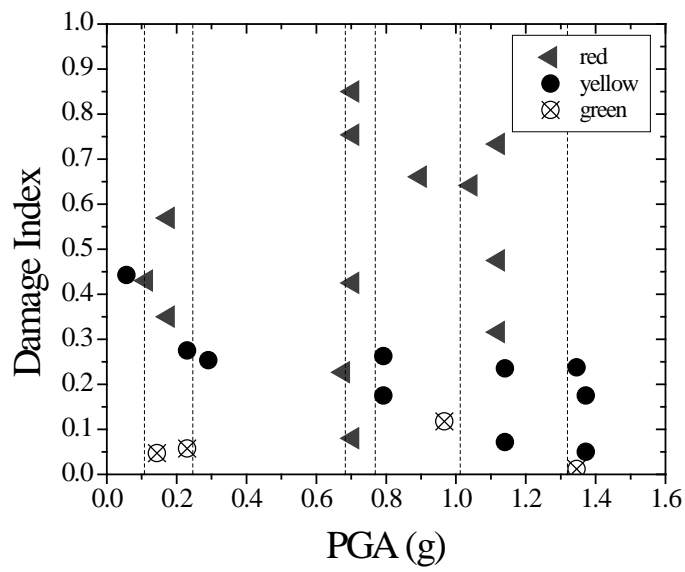


(h)

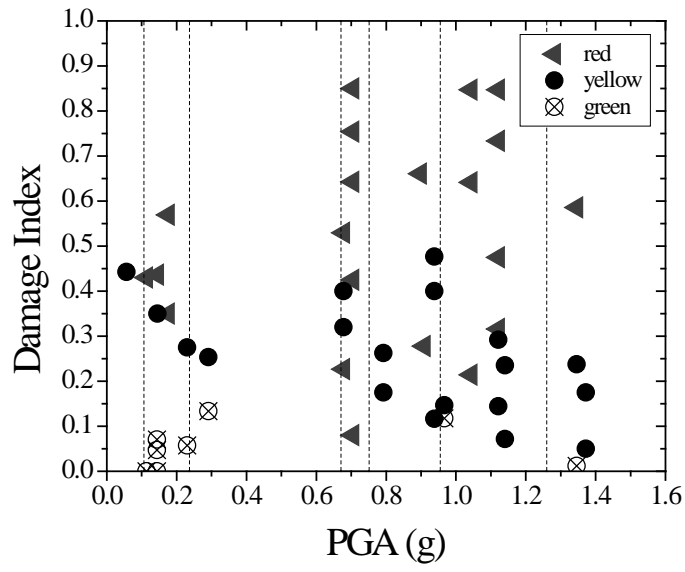
Figure 19 –Stone: (a) index 1: In-plane area ratio in the x (transversal) direction; (b) index 1: In-plane area ratio in the y (longitudinal) direction; (c) index 2: Area to weight ratio in the x (transversal) direction; (d) index 2: Area to weight ratio in the y (longitudinal) direction; (e) index 3: Base to shear ratio, taking cohesion into consideration, in the x (transversal) direction; (f) index 3: Base to shear ratio, taking cohesion into consideration, in the y (longitudinal) direction; (g) index 3: Base to shear ratio, considering zero cohesion, in the x (transversal) direction; (h) index 3: Base to shear ratio, considering zero cohesion, in the y (longitudinal) direction.



(a) Clay brick churches

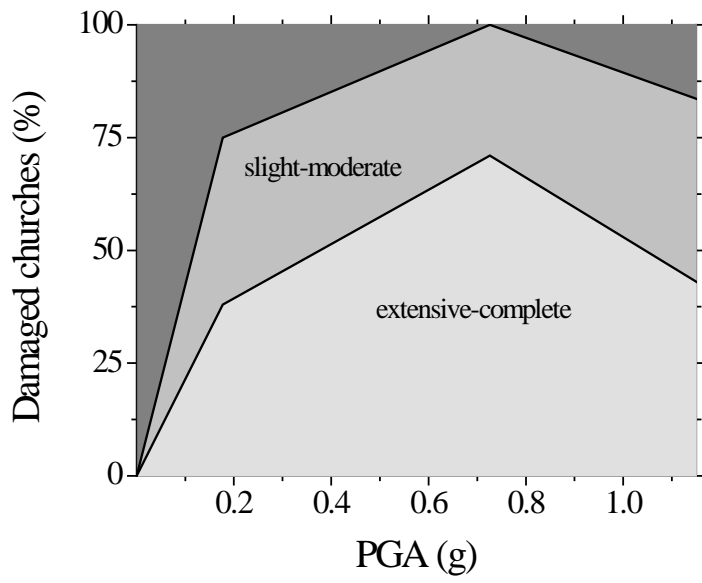


(b) Stone churches

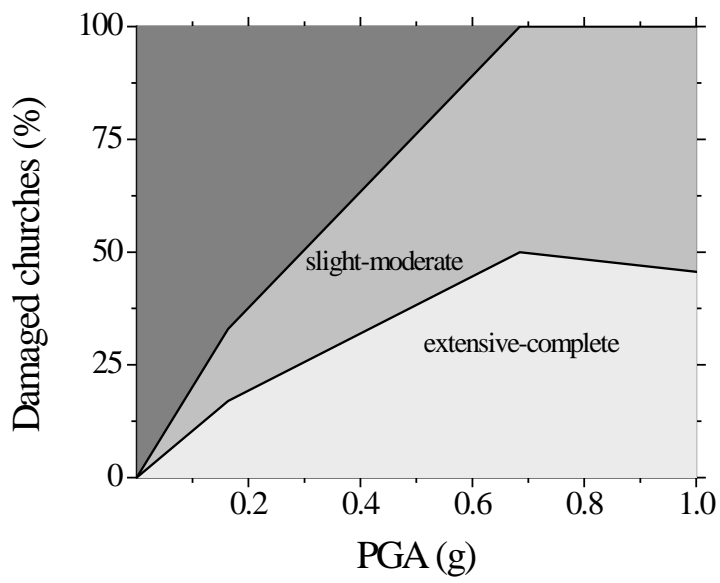


(c) All churches

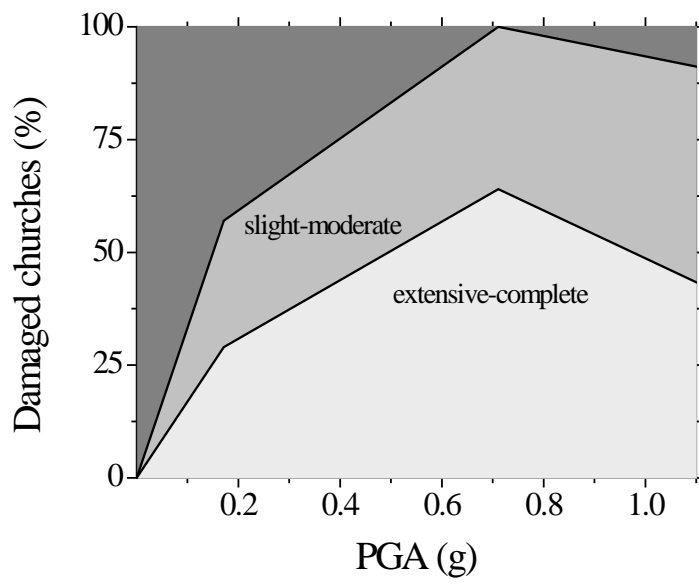
Figure 20 - Relation between damage index and PGA, with data clustering for the fragility curves.



(a)

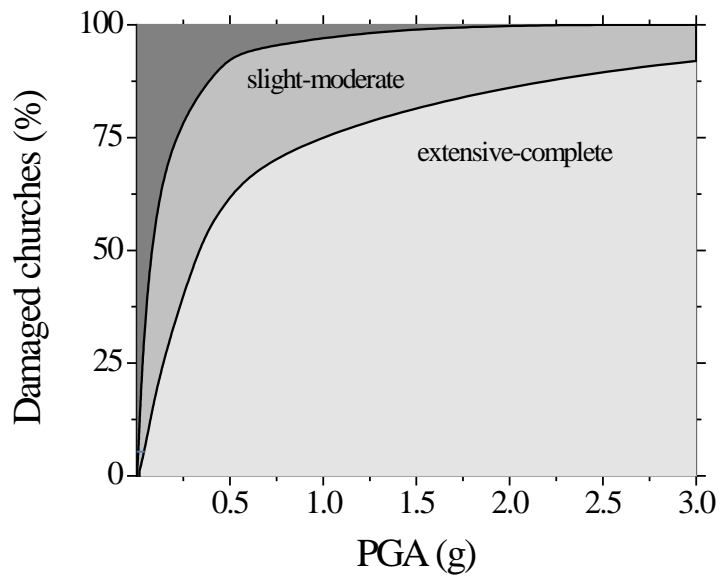


(b)

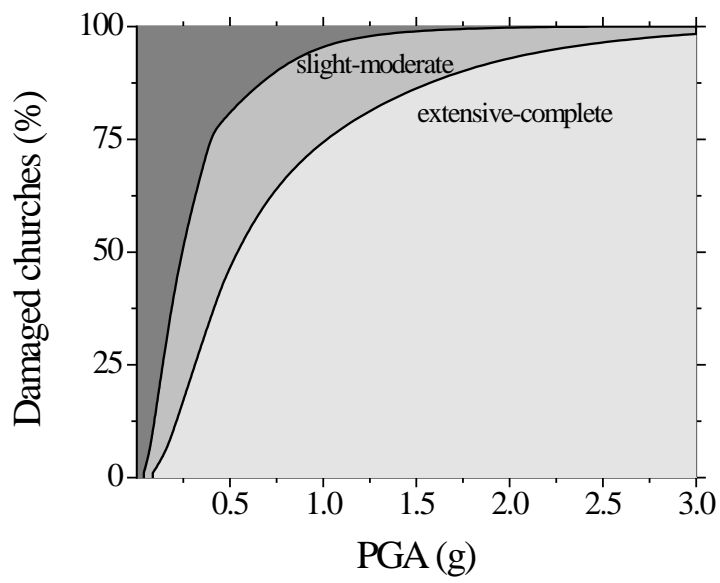


(c)

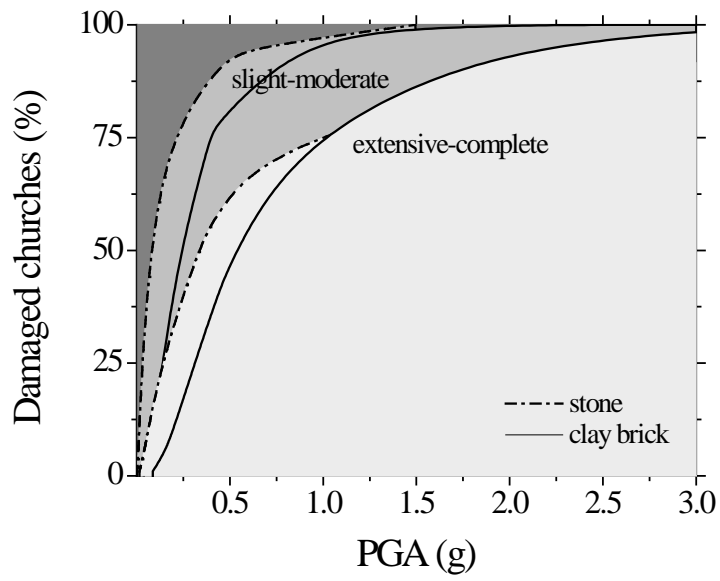
Figure 21 – Empirical fragility curves: (a) stone churches; (b) clay brick churches; (c) all churches.



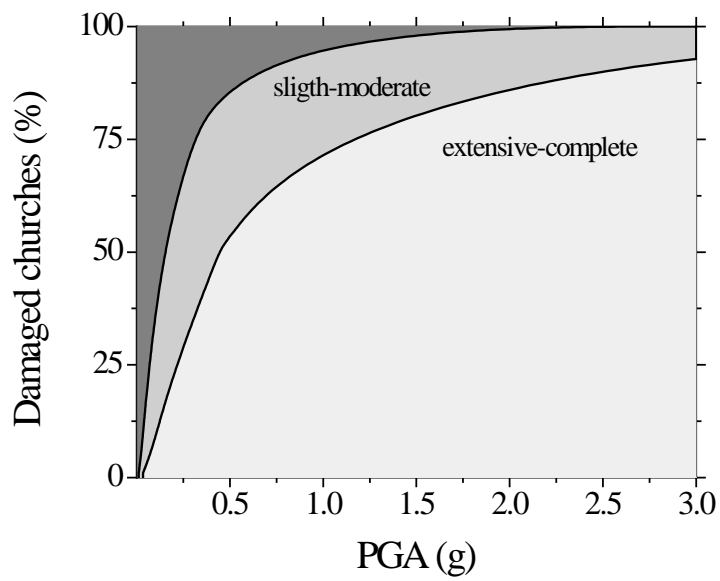
(a)



(b)



(c)



(d)

Figure 22 – Fragility curves: (a) stone churches; (b) clay brick churches; (c) stone and brick; (d) all churches.